JOURNAL OF AIRCRAFT
Vol. 45, No. 2, March–April 2008

# Experimental Investigation of Pairs of Vortex Filaments in Ground Effect

Linda K. Kliment* and Kamran Rokhsaz†
*Wichita State University, Wichita, Kansas 67260-0044*

DOI: 10.2514/1.32584

**The motion of corotating filaments in ground effect is investigated using a water tunnel. The vortices are generated using two flat blades and the ground is modeled with a splitter plate. The time history of the vortex motion is recorded at several downstream locations. Data are shown for two ground-plane positions and compared with the vortex behavior in the freestream. The experimental data are also compared with a potential-flow model. Results show that the vortices undergo a rebound as the result of ground effect. The vortices also undergo a lateral motion due to potential-flow effects. A leapfrogging behavior is present due to the differences in the lateral motions caused by the ground proximities of the spiraling vortices. In addition, the filaments form planar waves and move along preferred directions.**

## Nomenclature

| | | |
|---|---|---|
| $b$ | = | wing span |
| $b_0$ | = | vortex span at the trailing edge of the blades |
| $C$ | = | chord |
| $N$ | = | total number of vortices |
| $r$ | = | local vortex span |
| $Re_\Gamma$ | = | vortex Reynolds number, $\Gamma/\nu$ |
| $V_\infty$ | = | freestream velocity |
| $x, y, z$ | = | coordinate axes |
| $\dot{x}, \dot{y}, \dot{z}$ | = | velocities |
| $\alpha$ | = | angle of attack |
| $\Gamma$ | = | circulation |
| $\theta$ | = | inclination angle of the planar wave relative to the connecting line |
| $\omega$ | = | frequency of spiraling (orbiting rate) |

## I. Introduction

THE vortical flows in the wakes of heavy transport aircraft pose a great hazard to smaller vehicles, which can be upset dangerously when encountering them. This threat is the greatest in terminal areas in which

1) Large aircraft fly the slowest and produce the strongest vortices.
2) Aircraft of different sizes have to fly within the same airspace.
3) The traffic is most congested.
4) Aircraft are heaviest at takeoff.
5) Lower altitudes reduce the margin of safety required for recovery in case of an encounter. This danger assumes a new dimension very close to the ground, where wake vortices can also interact with the ground plane. These interactions can lead to their lateral and vertical motions in ways that are difficult to predict, at best.

In the absence of strong viscous effects, certain parallels can be drawn between the behavior of vortices in ground effect and the interactions between the two sides of a complete wake. A single vortex filament near the ground interacts with its own images and moves parallel to the ground in the same manner as a pair of counter-rotating vortices sink at altitude. Likewise, symmetric modes of motion of complex wakes are the same as those of pairs of filaments in ground effect if viscous effects are weak. For this reason, it may be helpful to briefly review the behavior of complete wake vortex systems without ground effect first.

Presented as Paper 3751 at the 36th AIAA Fluid Dynamics Conference, San Francisco, CA, 5–8 June 2006; received 2 June 2007; revision received 23 November 2007; accepted for publication 23 November 2007. 

*Research Assistant, Department of Aerospace Engineering. Student Member AIAA.
†Professor, Department of Aerospace Engineering. Associate Fellow AIAA.

## II. Physics of the Flow

### A. Outside of Ground Effect

Outside of ground effect (OGE), the dynamics and the natural aging of a pair of counter-rotating vortex filaments are well known. The understanding is that in the absence of atmospheric stratification, the pair sinks at a somewhat steady speed relative to the surrounding air mass. The primary means of dissipating the vortices is the unstable mutually induced motion [1], with the viscous effects contributing little to the process [2,3] except at small vortex spans in which the two viscous cores begin to interact [4].

Complex wakes, consisting of pairs of co- and counter-rotating filaments on each side, can exhibit additional modes of instability that can contribute to their self-destruction. Crouch [5], using an inviscid model, showed the possibility of nonlinear transient growth with amplification rates many times that of the Crow instability. Fabre and Jacquin [6] developed a similar inviscid model for vortices of unequal strength, paralleling the numerical investigations of Rennich and Lele [7]. In this case, two counter-rotating vortex filaments were placed on each side of the wake. They showed this configuration to have three unstable modes: two symmetric (one of which corresponds to the two-dimensional case) and one antisymmetric. For vortex strength ratios and relative spans used in this paper, the authors showed that one of the symmetric long-wave modes would exhibit growth rates 10 times those predicted by Crow [1]. Strong interaction was shown between the inner pair and the outer pair, but the most unstable case was shown to be associated with the short-wave instability of the inner pair of the vortices, leading to their destruction without impacting the motion of the outer vortices. Some of these results were also verified in a tow tank by Durston et al. [8]. They also showed the existence of transient growth, but with magnitudes much smaller than those shown by Crouch [5]. In [9], the authors extended this analysis later to include co- or counter-rotating vortices on each side, with similar results.

Investigation of complex wakes has also led to reexamination of the behavior of corotating filaments, typical of those emanating from wingtip and flap tip on one side of an aircraft [10–14], primarily emphasizing the mechanism for merging. Until recently, these configurations were deemed unconditionally stable within the context of inviscid flow [15]. However, recent analytical developments have raised questions concerning this issue [16].

Furthermore, in those cases in which there is viscous interaction between the cores, the development of short-wave instabilities within these structures has been shown analytically [17] and numerically [18]. Surprisingly, the literature is quite void of any information about the behavior of these structures near a solid boundary.

### B. Effects of Ground Proximity

There is a wealth of information available concerning the behavior of a pair of counter-rotating filaments near a ground plane. However, these studies have been divided into two categories, without direct connection between the two, perhaps because the differences in the background flow and or the relative importance of the viscous effects. In the first category, the emphasis has been placed on the effect of these structures on the nature and the behavior of the surface boundary layer. This type of flow has been investigated extensively in conjunction with formation of Gortler vortices leading to boundary-layer transition [19] and the nature of turbulent boundary layers, in which these structures are shown to appear and disappear at random [20].

The second category of problems, which is of interest in this paper, deals with aircraft wake vortex in ground proximity. In this context, the flowfields can be divided into three regimes, depending on the height of the wake. Although there is no consensus on the thickness of each region, there is agreement on the underlying behavior of the vortices in each layer. For the purpose of the following discussion, these regimes are defined in the same manner as in [21].

In the case of counter-rotating vortices, it is believed that at heights above approximately 1.5 times the initial vortex span $b_0$, there is very weak interaction between the trailing vortices and the ground. Therefore, the wake is said to be OGE and a counter-rotating pair of vortex filaments would sink at constant rate due to their mutual interaction. At these heights, the dynamics of the filaments is governed by their mutual interactions. Near ground effect (NGE) is defined at heights of about 1.5 to 0.5 times the vortex span, and the viscous interactions between a conventional wake consisting of two counter-rotating filaments and the ground are considered to be negligible. Therefore, the trailing vortices can be modeled by introducing an image pair below the ground level. At these heights, again, the dynamics of filament motion are dictated by the mutual interactions among the vortices and/or with their images. As the vortices sink below approximately half-span, they emerge into ground effect (IGE). In this region, they induce a crossflow on the ground that results in the formation of a thin boundary layer normal to the filaments. The adverse pressure gradient associated with this flow leads to the separation of this boundary layer, which in turn results in the release of additional vortices near the ground. The interaction between the main filaments and those due to boundary-layer separation causes the wake vortices to spiral near the ground. This is manifested as vortex rebound and can raise the main filaments above the ground by as much as two vortex spans. Consequently, any modeling of this type of flow must include the effect of viscosity.

Harvey and Perry [22] first suggested the connection between viscosity and rebounding of counter-rotating vortices that was verified by Orlandi [23]. He showed that on a no-slip boundary, a strong shear layer would form over the surface that would detach and form additional vortices. The interactions between these and the primary vortices would drive the latter away from the wall. Donnelly et al. [24] also used a pair of counter-rotating filaments in a water tank to show the same effects. These results were also confirmed by the two-dimensional numerical simulations of Zheng and Ash [25], who demonstrated surface boundary-layer separation in every case except at very high Reynolds numbers. Furthermore, they illustrated that at Reynolds numbers as high as 75,000, the filaments rebounded rapidly and reached heights twice those for the low-Reynolds number cases. Their solutions showed that the rebound vortices would assume a spiral-like shape, appearing to form a loop when viewed from downstream. The looping of the rebound vortex was also demonstrated by Hamilton and Proctor [26] and by Spalart et al. [27] using different numerical models. In the former paper, the authors employed a two-dimensional large eddy simulation and showed that in calm atmosphere, the lateral vortex position could oscillate by as much as one wing span. In the latter paper, a two-dimensional Reynolds-averaged Navier–Stokes solution was used to confirm that a single-pair rebound is due to the separation of the vortex-induced boundary layer and that the filaments loop in space. Their results also indicated that the *minimum* height of the rebound vortex would be approximately $0.56b_0$ for turbulent models and $0.65b_0$ for laminar models. Using a three-dimensional large eddy simulation, Proctor et al. [28] demonstrated that counter-rotating filaments could link with their images on the ground (Crow-type linking). This was also demonstrated analytically by Kornev and Reichert [29]. They observed pronounced vertical oscillations at lower levels of atmospheric turbulence and less vertical oscillations during rebound in the presence of high turbulence. Many of these characteristics have also been observed in natural environments using Doppler lidar (e.g., Kopp [30], Hallock and Burnham [31], and Burnham and Hallock [32]).

The technical literature is especially void of information concerning the interactions of corotating pairs of filaments with a ground plane. A transport aircraft on a takeoff run leaves behind pairs of corotating vortex filaments with spans comparable with the height above the ground. Although mutual induction does not force such a pair closer to the ground, one would expect the ground proximity to interfere with their merging and with their dissipation. Also, it is natural to believe that vortex rebound could occur in these cases, because the underlying flow physics is the same as that for counter-rotating filaments. Furthermore, it is possible for a pair of corotating filaments to interact with its image in the NGE layer and to exhibit some of the same instabilities as those of a complex wake.

Han and Cho [33] used a discrete vortex method to model the time-dependent development of a wake vortex sheet in ground effect. It is important to note that their aim was to investigate the development, and therefore the roll-up process, of the wake in ground proximity. Effects of viscosity were included in the vortex cores, but they assumed the flow to be inviscid in its interactions with the ground plane. Therefore, vortex rebound due to boundary-layer separation on the ground plane could not be predicted. When modeling a complex wake, their results indicated that a pair of corotating vortices would not spiral at the same rate near the ground as it would outside of ground effect. However, their conclusions were based on heights of less than 10% of the vortex span. Field measurements and computational fluid dynamics models of corotating filaments have shown that viscous interactions with the ground boundary layer prevent a wake from sinking so close to the ground.

The motion of corotating vortices near a plane of symmetry has also been studied in conjunction with the acoustics of leapfrogging vortex rings. The cross section of such a system resembles a pair of corotating filaments close to a slip boundary, interacting with its own image. Eldredge [34] investigated this flow using a two-dimensional direct numerical simulation solution and showed the shearing of the vortices, leading to eventual merger, to be very similar to that of the corotating pairs described by other authors. However, the slip plane of symmetry precluded correct modeling of vortex interaction with the boundary and prediction of rebound.

Laboratory investigations of co- or counter-rotating wake vortices in ground effect pose their own special challenges. A variety of techniques can be used to generate multiple longitudinal vortex filaments. However, modeling the interactions between the ground and the wake vortex can pose problems. In a tow tank [35], there is no natural boundary layer on the walls to simulate the shear layer due to the headwind in actual operations, whereas in wind tunnels and water tunnels, the natural boundary layers on the walls are too thick to be realistic. In some cases, the boundary layers are removed using suction or a moving wall [36]. However, in these cases, the crossflow shear layer that is responsible for vortex rebound is not modeled correctly.

The authors [37] previously demonstrated that a splitter plate can be used judiciously in a tunnel to simulate the surface boundary layer and to capture the essential features of such flowfields. In the present paper, the authors focus on the interactions of corotating wake

**Table 1 Parameters used in the experiments**

| Parameter | Value |
|---|---|
| Blade size | $20.57 \times 30.48 \times 0.16$ cm ($8.1 \times 12.0 \times 0.06$ in) |
| Blade separation | 5.08 cm (2.0 in.) |
| Angles of attack (blade 1, blade 2) | 9.5, 9.0 deg. |
| Flow speed | 8.53 cm/s (0.28 ft/s) |
| Data recorded at downstream locations, $x/b_0$ | 2.74, 5.49, 8.23, 10.97, 13.72, 16.46, 19.20, 21.95, 24.69, 27.43 |
| Vortex span, $b_0$, at $x/b_0 = 2.74$ | 5.56 cm (2.19 in.) |
| Vortex strengths (vortex 1, vortex 2) | 24.62, 22.39 $cm^2/s$ (0.0265, 0.0241 $ft^2/s$) |
| Vortex Reynolds number (vortex 1, vortex 2) | 2190, 1992 |
| Orbiting rate | |
| Case 1 | 0.205 rad/s |
| Case 2 | 0.214 rad/s |
| Case 3 | 0.179 rad/s |
| Ground plane's leading edge | |
| Case 1 | None |
| Case 2 | 15.2 cm (6.0 in.), $x/b_0 = 5.49$ |
| Case 3 | 45.7 cm (18.0 in.), $x/b_0 = 10.97$ |

vortices with the ground plane. Of special interest is the influence of the ground proximity on the dynamic behavior of such vortex filaments. When appropriate, comparisons are also made with numerical predictions for such flows.

## III. Experimental Method

### A. Test Facility

The experiments were performed in a closed-loop horizontal water tunnel. This facility contained approximately 13,250 liters (3500 gal) of water. The test section measured 0.6 m (2 ft) wide, 0.9 m (3 ft) high, and 1.8 m (6 ft) long and was visible from five different directions. Water speeds could vary from 1.52 cm/s (0.05 ft/s) to 30.48 cm/s (1.0 ft/s). For these experiments, the tunnel speed was 8.23 cm/s (0.27 ft/s). This speed was chosen because it had the lowest levels of freestream turbulence and tunnel vibration. The flow was visualized by dye injection.

### B. Test Apparatus

Vortex filaments were generated with two rectangular flat blades for which the specifications are given in Table 1. These blades were mounted on a reflection plane that measured 30.5 cm (12 in.) wide and 28.3 cm (11.1 in.) long and that was attached to the sidewall of the tunnel 3.81 cm (1.5 in.) from the wall. The point between the blade quarter-chords was 47.6 cm (18.75 in.) below the top of the tunnel. This reflection plane setup allowed individual control of the vortex strengths and spans, because the blades' angles and separation distances could be set independently. For the results included in this paper, the separation distance between the blades' quarter-chords was 5.08 cm (2 in.). The result of this blade separation was a vortex span of 5.56 cm (2.19 in.) at the trailing edge of the vortex generators.

To eliminate the effects of the boundary layer on the tunnel wall, a splitter plate was added to the test section to model the ground. This plate was placed 20.5 cm (8.1 in.) from the tunnel wall and parallel to it, on the opposite side of the reflection plane. The results from two cases with the ground plane, as well as one case without, are included in this paper. In one case, the leading edge of the ground plane was 15.24 (6 in.) downstream of the trailing edge of the blades, whereas it was moved to 45.72 cm (18 in.) for the next case. In both cases, the distance between the surface of the ground plane and the tips of the vortex generators was 6.19 cm (2.44 in.). Data were acquired at 15.2-cm (6-in.) increments downstream of the blades, starting at the trailing edge. The setup, shown in Figs. 1 and 2, was identical to that used in [37], except that the blades were mounted on a smaller reflection plane and were angled to produce corotating vortices in this case.

### C. Data Acquisition

The data acquisition was identical to that reported by Rokhsaz and Kliment [14] and is described briefly here. A water–milk–alcohol mixture was injected in the vortex core near the leading edge of the blades. A white light sheet was positioned perpendicular to the test section at the downstream location at which the data were being recorded. All surrounding lights were turned off so that everything was dark except the dye mixture at the position at which it was intersected by the light sheet. A video camera was placed downstream of the test section, pointed upstream toward the vortex generators. From this viewpoint, the illuminated vortex cross sections appeared as bright spots against a dark background. This was digitally recorded at the rate of 30 Hz for 2.5 min. The time and position information was determined for each frame of the video. In addition to the kinematics information, the preferred direction of vortex motion was found from the second moments of the instantaneous positions relative to the mean vortex location.

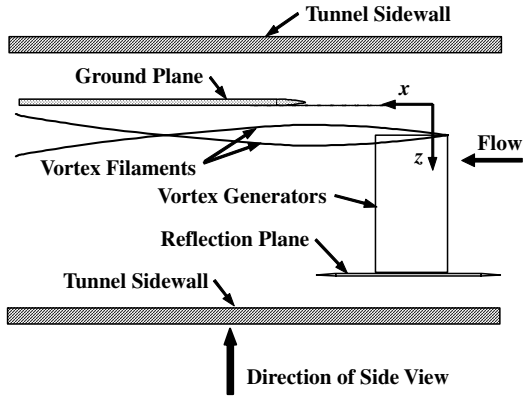


**Fig. 1 Schematic top view of the test section.**

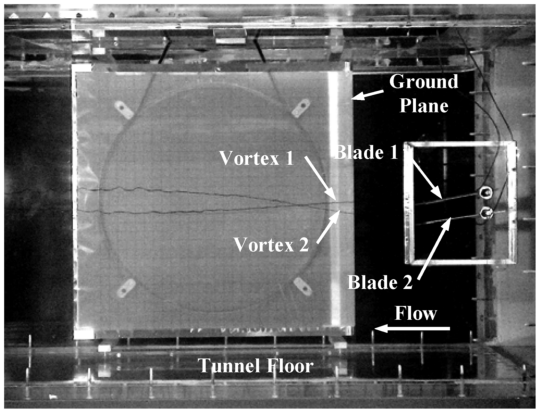


**Fig. 2 Side view of the test section.**

## IV. Numerical Model

The flowfield was divided into two regions, depending on the proximity of the ground plane. The vortices were assumed to be OGE in the absence of the ground plane and upstream of it when it was present in the tunnel. IGE, the flow was modeled using images of the filaments below the ground plane. Therefore, interactions between the vortices and the ground plane were purely due to potential flow. Even though the experimental data showed some vortex rebound due to ground-boundary-layer separation, there was no rational way of modeling the release of the secondary vortices [38] into the flowfield to model this effect.

The vortex positions in the $y$–$z$ plane were found from the solution of a set of simultaneous differential equations and the system was assumed to be convected downstream by the freestream. Using the classical method outlined by Hassan [39], the following Hamiltonian described the motion of the point vortices in an otherwise stationary body of fluid:

$$H = -\sum_{\substack{i=1\\ j=i+1}}^{N} \frac{\Gamma_i \Gamma_j}{2\pi} \ell_n[\sqrt{(z_j - z_i)^2 + (y_j - y_i)^2}] \tag{1}$$

where $N$ was the total number of vortices. From this expression, the canonical equations of motion were obtained from

$$\Gamma_i \dot{y}_i = \frac{\partial H}{\partial z_i} \tag{2}$$

and

$$\Gamma_i \dot{z}_i = -\frac{\partial H}{\partial y_i} \tag{3}$$

In the OGE regime, $N = 2$, and so this process resulted in four simultaneous differential equations. The vortices were assumed to enter IGE when they arrived over the ground plane. Addition of the images below the ground plane resulted in eight simultaneous differential equations. These equations were solved using a fourth-order Runge–Kutta [38] scheme. The starting coordinates of the vortices were obtained from experimental data. Therefore, in subsequent comparisons between the numerical and the experimental data, perfect agreement can be seen at the start.

## V. Results and Discussion

### A. Experimental Results

Experimental data were collected for three cases: 1) without the ground plane, 2) with the ground plane's leading edge 15.24 cm (6 in.) downstream of the blades' trailing edges, and 3) with the ground plane's leading edge at 45.72 cm (18 in.) downstream. The coordinate system used for the experimental data is shown schematically in Fig. 1. The origin of this coordinate system was placed at the quarter-chord of the vortex generators on the ground plane. Therefore, in the discussions to follow, all heights are measured relative to the ground plane. Also, all vortex trajectories shown and discussed in subsequent sections were time-averaged. Finally, the reader is cautioned that all the position plots shown here are highly distorted. In the interest of clarity, the scales used for the lateral and vertical positions were magnified approximately 10 times compared with that used for the streamwise direction. Consequently, the errors in these results also appear to be 10 times larger than they are.

The vertical position of the vortices as a function of the downstream position is shown in Fig. 3 for all three cases. In this figure, the vortex position in the absence of the ground plane can be used for reference. The results shown in this figure point to the occurrence of vortex rebound as the result of ground effect. Both cases 2 and 3 closely followed the results of case 1 until the flow reached the leading edge of the ground plane ($x/b_0 = 5.49$ for case 2 and 10.97 for case 3). The authors speculate that this rebound is exactly the same in nature as that described earlier in connection with a pair of counter-rotating vortices. However, unlike in the counter-rotating case, corotating vortices were not driven toward ground by mutually induced velocities. Therefore, they remained farther away from the ground, resulting in a somewhat weaker rebound.

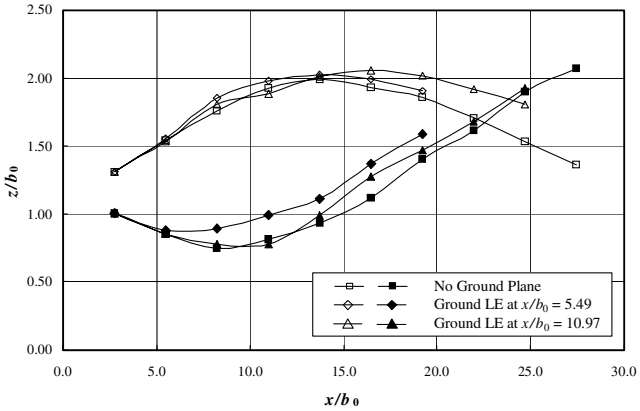


**Fig. 3 Vertical vortex position.**

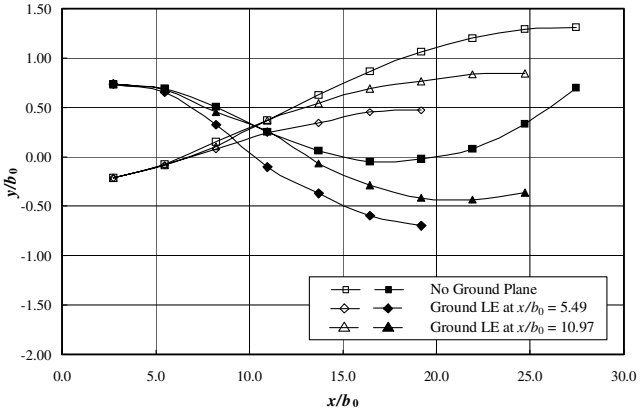


**Fig. 4 Lateral vortex position.**

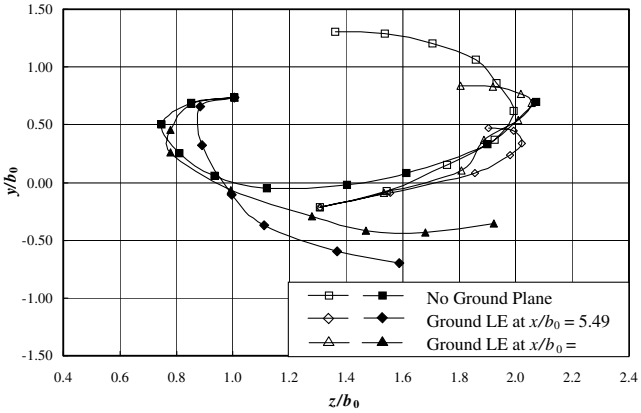


**Fig. 5 Downstream view of the vortices.**

The influence of ground effect on the lateral vortex position is shown in Fig. 4. Again, the results of cases 2 and 3 followed those of case 1 closely until the vortices arrived over the ground plane. Beyond this point, the interactions between the vortices and their images resulted in the lateral motion that is clearly evident in this figure. This is purely a potential-flow effect and can also be seen clearly in the downstream view of the wake given in Fig. 5. From this viewpoint, the vortices orbit in the clockwise direction, all starting from the same location (i.e., the trailing edge of the blades). However, after one half-orbit, significant differences in the lateral vortex positions were introduced by the ground proximity. The

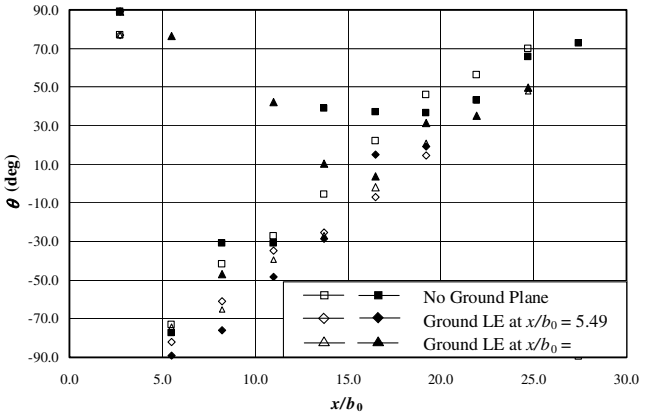


**Fig. 6 Preferred direction of motion.**

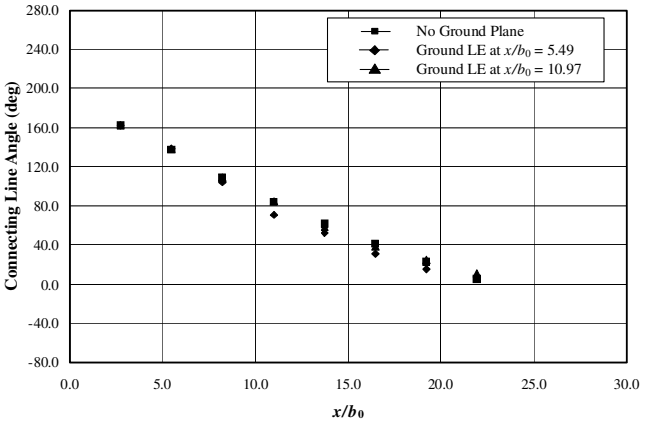


**Fig. 7 Connecting line angle showing the spiraling rate.**

combination of this motion and the natural spiraling of the filaments led to the appearance of leapfrogging when viewed from this perspective. This behavior is very similar to that described by Eldredge [34] and others in connection with the motion of corotating vortex rings. This issue will be discussed further in a later section.

Previously, the authors have reported on the tendency of corotating vortex filaments to undergo planar oscillatory motion along preferred directions [13,14,16]. However, of interest in this case was the influence of ground effect on this behavior. Figure 6 shows the inclination angle of the preferred direction of motion relative to the line connecting the mean vortex positions. It is obvious from this figure that these angles changed rather monotonically with increasing downstream distance, without any discernible impact from the presence of the ground plane. Likewise, ground effect on the orbiting rate of the vortices was small, as demonstrated in Fig. 7. This figure shows the orientation of the line connecting the mean positions of the vortices at each downstream location. Therefore, the slope of this line is directly proportional to the orbiting rate of the filaments.

### B. Comparison with Numerical Results

Examination of the results shown in Fig. 4 reveals a slight drift in the data caused by the tunnel, corresponding to a slight flow curvature in the vertical direction in the absence of the ground plane. The authors believe that this was caused by the slight blockage introduced asymmetrically in the tunnel by the presence of the test apparatus. Subtracting the drift from the vertical position of the filaments resulted in excellent agreement between the experimental and numerical results, as shown in Fig. 8. The maximum position error, defined by $\Delta z/\Delta x$, was reduced to less than 1%.

A similar deviation from straight-line flow was also present in the lateral direction, as shown in Fig. 5. The average side deviation in velocity (i.e., crossflow) was estimated to be 0.383 cm/s

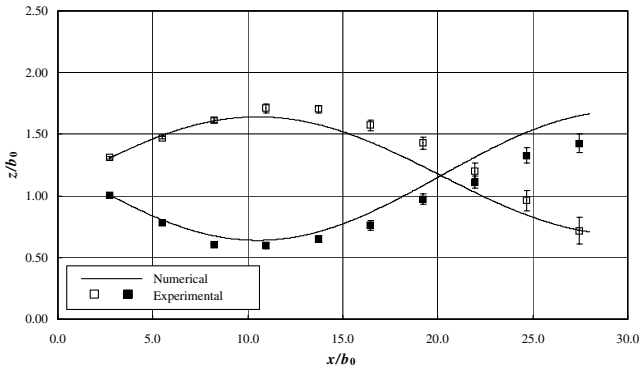


**Fig. 8 Vertical positions without ground effect.**

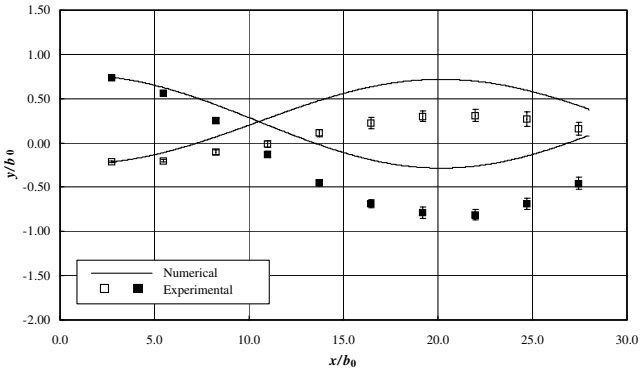


**Fig. 9 Lateral positions without ground effect.**

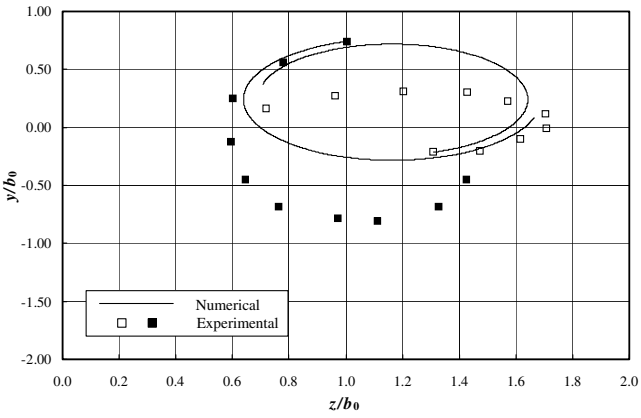


**Fig. 10 Downstream view of vortex positions without ground effect.**

(0.0126 ft/s), corresponding to a 5.5-kt crosswind on a 120-kt approach speed. However, this was not a linear deviation and although subtracting it from the lateral positions did result in better agreement between the two sets of results, it did not uniformly reduce the differences between the two, as indicated in Figs. 9 and 10. The maximum position error in this case, defined by $\Delta y/\Delta x$, remained closer to 3%. The authors believe that the main source of this deviation was the water-tunnel wall effect. The tips of the vortex generators were closer to the far sidewall of the tunnel, creating a slightly stronger interaction with that wall. Because the splitter plate, simulating the ground plane, was to be introduced on that side, the authors did not believe this drift to be a serious issue.

In the presence of ground effect, much better agreement was obtained between the numerical and the experimental data. These results are shown in Figs. 11–16. Figures 11–13 show the results of case 2, in which the ground plane's leading edge was 15.24 cm (6 in.) downstream of the blades' trailing edges. Figures 14–16 show the

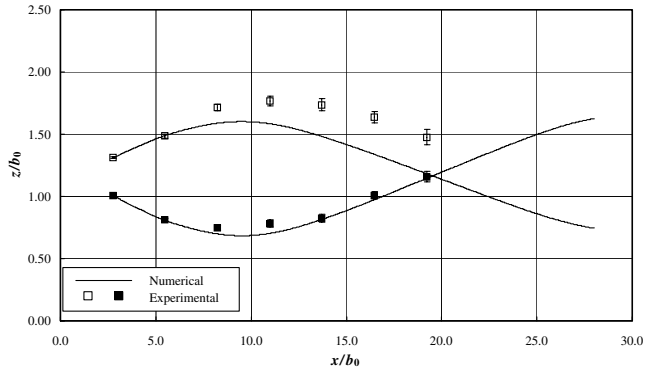


**Fig. 11 Vertical position, $x/b_0 = 5.49$.**

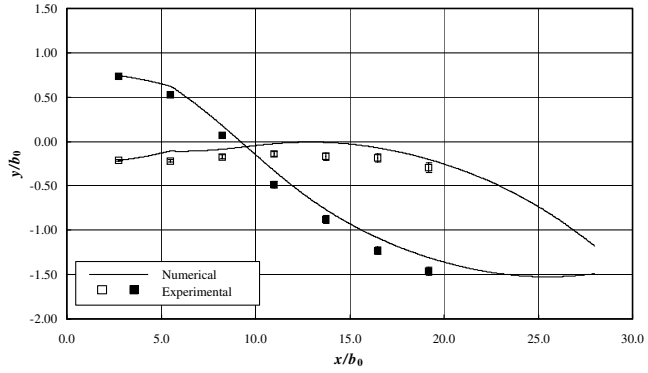


**Fig. 12 Lateral position, $x/b_0 = 5.49$.**

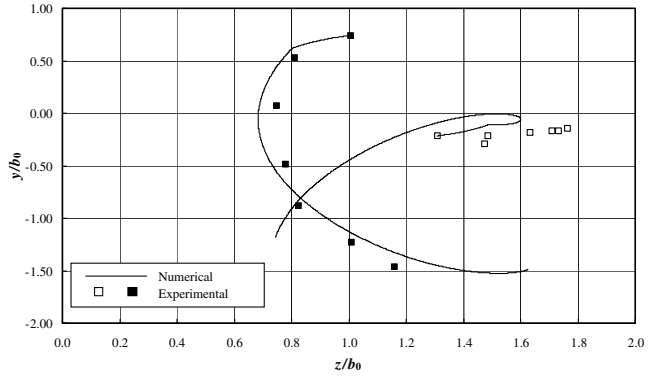


**Fig. 13 Downstream view, $x/b_0 = 5.49$.**

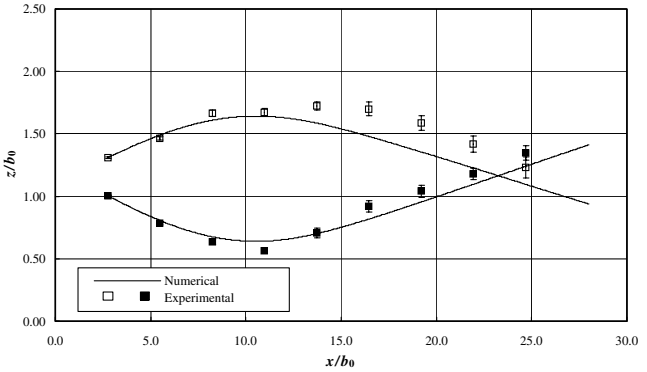


**Fig. 14 Vertical position, $x/b_0 = 10.97$.**

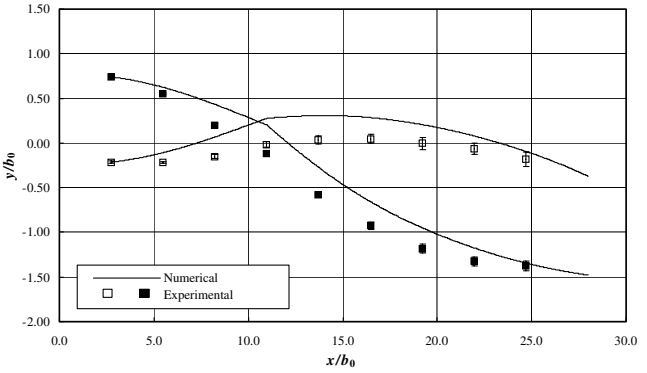


**Fig. 15 Lateral position, $x/b_0 = 10.97$.**

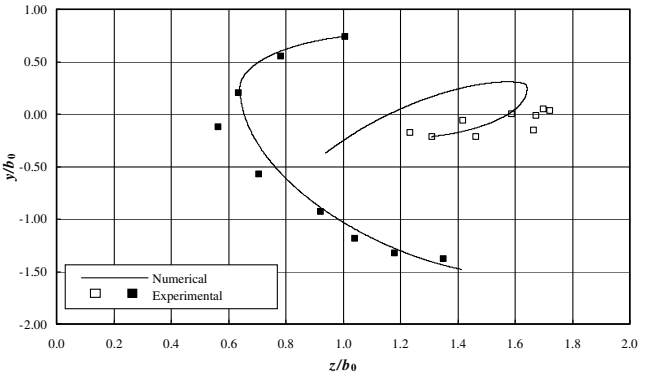


**Fig. 16 Downstream view, $x/b_0 = 10.97$.**

same results for case 3 with the ground plane starting at 45.7 cm (18 in.) downstream.

The vertical vortex positions are shown in Figs. 11 and 14. The rebound that was discussed earlier is clearly visible in both figures, starting at the leading edge of the ground plane. The experimental data indicate that the vortices began to rise above the ground plane. This behavior is due to boundary-layer separation on the ground plane, leading to release of secondary vortices from the ground. Robins and Delisi [21] suggested a simple way of modeling this phenomenon for counter-rotating vortices. They tuned the initial position and the strength of the secondary vortices in their numerical model by using a large amount of experimental data collected in the field using lidar. However, in the absence of such a database for corotating vortices, it was not possible to construct such a model in this case.

The lateral vortex positions are presented in Figs. 12 and 15. Much better agreement between the experimental data and the numerical results is quite evident in these figures. It is obvious that as long as the vortices were outside of ground effect (i.e., upstream of the ground plane), they spiraled normally. However, once over the ground plane, their lateral positions were influenced strongly by their images. This lateral motion resulted in a leapfrogging motion that was very similar to that of corotating vortex rings, discussed by Eldrege [34] and others. This form of motion is further obvious when considering the downstream views, shown in Figs. 13 and 16. It is evident from these figures that as the result of ground effect, the upper vortex remained nearly stationary in the lateral direction, whereas the lower vortex moved rapidly under it. Had data been collected farther downstream, it would have been clear that the two vortices would switch positions eventually. This type of motion is in quite a contrast with that outside of ground effect, shown in Fig. 10.

Using their numerical model, Han and Cho [33] showed that the distance between the vortices (i.e., vortex span) would vary significantly as a function of downstream position. This variation was also detected in the experimental data and supported by the numerical results. One case is shown in Fig. 17. However, the degree of variation in the vortex span was not as large as they predicted. The

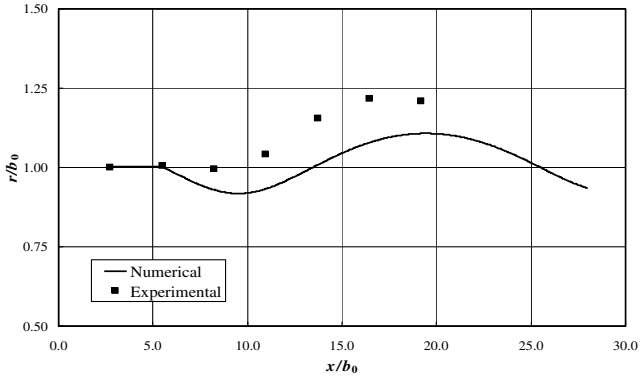


**Fig. 17 Vortex span in ground effect, $x/b_0 = 5.49$.**

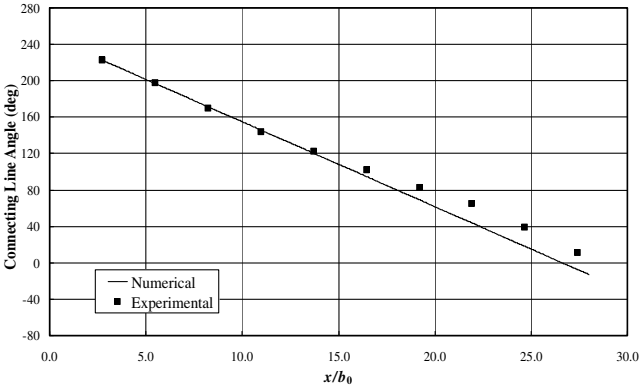


**Fig. 18 Spiraling without ground effect.**

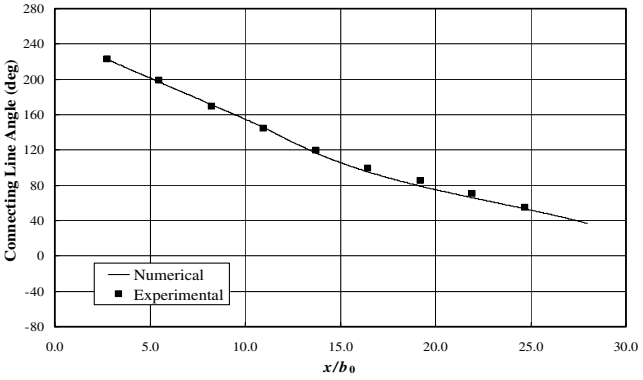


**Fig. 19 Spiraling with ground plane at $x/b_0 = 10.97$.**

authors attribute the differences to the unrealistically small heights used by Han and Cho.

Ground effect on the spiraling rate of the line connecting the mean vortex positions is shown in Figs. 18 and 19. Comparison of these figures reveals that ground effect changed the spiraling rate slightly. The reader is cautioned that the spiraling rate is the slope of the given curves. Whereas without ground effect, the spiraling rate remained rather constant, addition of the ground plane reduced this quantity. In light of the leapfrogging behavior that was discussed earlier, this was an expected outcome.

The results discussed in the preceding summary show very good agreement between the numerical model and experimental data. This is with the exception of the unexplained asymmetry of the lateral position in the absence of ground effect. All of the significant features of the flow can be seen in both sets of data. Even though other corroborating data are absent in the technical literature, this level of agreement between the two methods tends to support the conclusions drawn in this paper.

## VI. Conclusions

The dynamic interactions of pairs of corotating vortex filaments were explored in ground effect. The experimental data were acquired in a water tunnel in which the time history of the motion of the filaments was recorded. From this data, the vertical and the lateral mean vortex positions were deduced over a distance of approximately 25 span lengths. Of special interest was the interaction of such a pair of filaments with the ground plane.

In the absence of similar results in the open literature, a potential-flow model was used to cross-check the experimental results. All of the salient features of the flow could be detected in both methods. Furthermore, it was shown that

1) Within these heights, and for the vortex spans considered here, very good agreement was shown between a potential-flow model and the experimental results.

2) The vortices exhibited rebound as the result of ground effect, possibly due to crossflow boundary-layer separation on the ground plane. This was completely consistent with the results shown earlier for counter-rotating filaments.

3) Ground effect induced a lateral motion on the filaments, consistent with potential-flow theory. This in turn created a leapfrogging motion in the lateral direction.

4) Lateral leapfrogging caused cyclic changes in the vortex span.

5) The presence of the ground did not alter the preferred direction of motion of the vortices.

6) Ground effect had no discernible effect on the vortex spiraling rate.

## References

[1] Crow, S. C., "Stability Theory for a Pair of Trailing Vortices," *AIAA Journal*, Vol. 8, No. 12, Dec. 1970, pp. 2172–2179.

[2] Greene, G. C., "An Approximate Model of Vortex Decay in the Atmosphere," *Journal of Aircraft*, Vol. 23, No. 7, 1986, pp. 566–573.

[3] Hallock, J. N., and Burnham, D. C., "Decay Characteristics of Wake Vortices from Jet Transport Aircraft," 35th AIAA Aerospace Sciences Meeting and Exhibit, Reno, NV, AIAA Paper 97-0060, Jan. 1997.

[4] Laporte, F., and Leweke, T., "Elliptic Instability of Counter-Rotating Vortices: Experiment and Direct Numerical Simulation," *AIAA Journal*, Vol. 40, No. 12, Dec. 2002, pp. 2483–2494.

[5] Crouch, J. D., "Instability and Transient Growth for Two Trailing-Vortex Pairs," *Journal of Fluid Mechanics*, Vol. 350, Nov. 1997, pp. 311–330.
doi:10.1017/S0022112097007040

[6] Fabre, D., and Jacquin, L., "Stability of a Four-Vortex Wake Model," *Physics of Fluids*, Vol. 12, No. 10, Oct. 2000, pp. 2438–2443.

[7] Rennich, S. C., and Lele, S. K., "Method for Accelerating the Destruction of Aircraft Wake Vortices," *Journal of Aircraft*, Vol. 36, No. 2, Mar.–Apr. 1999, pp. 398–404.

[8] Durston, D. A., Walker, S. M., Driver, D. M., and Smith, S. C., "Wake-Vortex Alleviation Flowfield Studies," *Journal of Aircraft*, Vol. 42, No. 4, July–Aug. 2005, pp. 894–907.

[9] Fabre, D., Jacquin, L., and Loof, A., "Optimal Perturbations in a Four-Vortex Aircraft Wake in Counter-Rotating Configuration," *Journal of Fluid Mechanics*, Vol. 451, Jan. 2002, pp. 319–328.

[10] Jacob, J. D., "Experimental Investigation of Corotating Trailing Vortices," Proceedings of 36th Aerospace Sciences Meeting and Exhibit, Reno, NV, AIAA Paper 98-0590, Jan. 1998.

[11] Jacob, J. D., "Experiments on Trailing Vortex Merger," Proceedings of 37th Aerospace Sciences Meeting and Exhibit, Reno, NV, AIAA Paper 99-0547, Jan. 1999.

[12] Jacob, J. D., and O. Savas, "Vortex Dynamics in Trailing Wakes of Flapped Rectangular Wings," 35th Aerospace Sciences Meeting and Exhibit, Reno, NV, AIAA Paper 97-0048, Jan. 1997.

[13] Kliment, L. K., "Experimental Investigation of Flap Tip and Wing Tip Vortex Interactions," M.S. Thesis, Wichita State Univ., Wichita, KS, Dec. 2002.

[14] Rokhsaz, K., and Kliment, L. K., "Experimental Investigation of Corotating Vortex Filaments in a Water Tunnel," 32nd AIAA Fluid Dynamics Conference, St. Louis, MO, AIAA Paper 2002-3303, June 2002.

[15] Jimenez, J., "Stability of a Pair of Corotating Vortices," *Physics of Fluids*, Vol. 18, No. 11, Nov. 1975, pp. 1580–1581.
doi:10.1063/1.861056

[16] Miller, T. S., Kliment, L. K., and Rokhsaz, K., "Dynamics of Corotating Vortex Filaments, Part 1: Analytical Mode," *Journal of Aircraft* (to be published).
[17] Le Dizès, S., and Laporte, F., "Theoretical Predictions for the Elliptical Instability in a Two-Vortex Flow," *Journal of Fluid Mechanics*, Vol. 471, Nov. 2002, pp. 169–201. doi:10.1017/S0022112002002185
[18] Laporte, F., and Corjon, A., "Direct Numerical Simulations of the Elliptic Instability of a Vortex Pair," *Physics of Fluids*, Vol. 12, No. 5, May 2000, pp. 1016–1031.
[19] White, F. M., *Viscous Fluid Flow*, 3rd ed., McGraw–Hill, New York, 2006, pp. 368–370.
[20] Cullen, L. M., Han, G., Zhou, M. D., and Wygnanski, I., "On the Role of Longitudinal Vortices in Turbulent Flow over a Curved Surface," AIAA 1st Flow Control Conference, St. Louis, MO, AIAA Paper 2002-2828, June 2002.
[21] Robins, R. E., and Delisi, D. P., "NWRA AVOSS Wake Vortex Prediction Algorithm Version 3.1.1," NASA CR-2002-211746, June 2002.
[22] Harvey, J. K., and Perry, F. J., "Flowfield Produced by Trailing Vortices in the Vicinity of the Ground," *AIAA Journal*, Vol. 9, No. 8, 1971, pp. 1659–1660.
[23] Orlandi, P., "Vortex Dipole Rebound from a Wall," *Physics of Fluids*, Vol. 2, No. 8, Aug. 1990, pp. 1429–1436.
[24] Donnelly, M. J., Vlachos, P., and Telionis, D. P., "A Vortex Pair Impinging on a Solid Boundary," 36th Aerospace Sciences Meeting and Exhibit, Reno, NV, AIAA Paper 1998-690, Jan. 12–15, 1998.
[25] Zheng, Z. C., and Ash, R. L., "Study of Aircraft Wake Vortex Behavior Near Ground," *AIAA Journal*, Vol. 34, No. 3, Mar. 1996, pp. 580–589.
[26] Hamilton, D. W., and Proctor, F., "Wake Vortex Transport in Proximity to the Ground," *Proceedings of the 19th Digital Avionics Systems Conferences*, 7–13 Oct. 2000, Vol. 1, pp. 3E5/1–3E5/8.
[27] Spalart, P. R., Strelets, M. Kh., Travin, A. K., and Shur, M. L., "Modeling the Interactions of a Vortex Pair with the Ground," *Fluid Dynamics*, Vol. 36, No. 6, 2001, pp. 899–908. doi:10.1023/A:1017958425271
[28] Proctor, F. H., Hamilton, D. W., and Han, J., "Wake Vortex Transport and Decay in Ground Effect: Vortex Linking with the Ground," 38th Aerospace Sciences Meeting and Exhibit, Reno, NV, AIAA Paper 2000-0757, Jan.2000.
[29] Kornev, N. V., and Reichert, G., "Three-Dimensional Instability of a Pair of Trailing Vortices near the Ground," *AIAA Journal*, Vol. 35, No. 10, Oct. 1997, pp. 1667–1669.
[30] Kopp, F., "Doppler Lidar Investigation of Wake Vortex Transport Between Closely Spaced Parallel Runways," *AIAA Journal*, Vol. 32, No. 4, Apr. 1994, pp. 805–810.
[31] Hallock, J. N., and Burnham, D. C., "Decay Characteristics of Wake Vortices from Jet Transport Aircraft," 35th AIAA Aerospace Sciences Meeting and Exhibit, Reno, NV, AIAA Paper 97-0060, Jan.1997.
[32] Burnham, D. C., and Hallock, J. N., "Measurements of Wake Vortices Interacting with the Ground," 36th AIAA Aerospace Sciences Meeting and Exhibit, Reno, NV, AIAA Paper 98-0593, Jan. 1998.
[33] Han, C., and Cho, J., "Unsteady Trailing Vortex Evolution Behind a Wing in Ground Effect," *Journal of Aircraft*, Vol. 42, No. 2, Mar.–Apr. 2005, pp. 429–434.
[34] Eldredge, J. D., "The Acoustics of Two-Dimensional Leapfrogging Vortices," 11th AIAA/CEAS Aeroacoustics Conference, Monterey, CA, AIAA Paper 2005-2954, May 2005.
[35] Liu, H. T., and Srnsky, R. A., "Laboratory Investigation of Atmospheric Effects on Vortex Wakes," Flow Research, Inc., Rept. 497, Belleville, WA, 1990.
[36] Pailhas, G., Touvet, Y., and Barricau, P., "Instabilities Developing in a Wing Tip Counter-Rotating Vortex Pair: Experimental Evidence and Control," *Principles of Wake Vortex Alleviation Devices*, ONERA, Toulouse, France, Feb. 2005; available online at http://www.onecert.fr/projets/WakeNet2-Europe/wg7/dataProgrammeFeb05/day3/WG7_PRF_Pailhas_Web.pdf.
[37] Rokhsaz, K., and Kliment, L. K., "Feasibility of Modeling Wake Vortices in Ground Effect in a Water Tunnel," SAE AeroTech Congress and Exhibit, Grapevine, TX, Society of Automotive Engineers Paper 2005-01-3360, Oct. 2005.
[38] James, M. L., Smith, G. M., and Wolford, J. C., *Applied Numerical Methods for Digital Computation with FORTRAN and CSMP*, Harper & Row, New York, 1977, pp. 397–419.
[39] Hassan, A., "Motion of Three Vortices," *Physics of Fluids*, Vol. 22, No. 3, Mar. 1979, pp. 393–400.